Large reversible magnetocaloric effect induced by metamagnetic transition in antiferromagnetic HoNiGa compound*

Yi-Xu Wang(王一旭)[1], Hu Zhang(张虎)[1,†], Mei-Ling Wu(吴美玲)[1], Kun Tao(陶坤)[1], Ya-Wei Li(李亚伟)[1], Tim Yan(颜天宝)[2], Ke-Wen Long(龙克文)[2], Teng Long(龙腾)[1], Zheng Pang(庞铮)[1], and Yi Long(龙毅)[1]

[1] *School of Materials Science and Engineering, University of Science and Technology of Beijing, Beijing* 100083, *China*
[2] *ChuanDong Magnetic Electronic Co. Ltd., FoShan* 528513, *China*

(Received 29 July 2016; revised manuscript received 20 September 2016; published online 15 November 2016)

The magnetic properties and magnetocaloric effects (MCE) of HoNiGa compound are investigated systematically. The HoNiGa exhibits a weak antiferromagnetic (AFM) ground state below the Néel temperature T_N of 10 K, and the AFM ordering could be converted into ferromagnetic (FM) ordering by external magnetic field. Moreover, the field-induced FM phase exhibits a high saturation magnetic moment and a large change of magnetization around the transition temperature, which then result in a large MCE. A large $-\Delta S_M$ of 22.0 J/kg K and a high *RC* value of 279 J/kg without magnetic hysteresis are obtained for a magnetic field change of 5 T, which are comparable to or even larger than those of some other magnetic refrigerant materials in the same temperature range. Besides, the $\mu_0 H^{2/3}$ dependence of $|\Delta S_M^{pk}|$ well follows the linear fitting according to the mean-field approximation, suggesting the nature of second-order FM–PM magnetic transition under high magnetic fields. The large reversible MCE induced by metamagnetic transition suggests that HoNiGa compound could be a promising material for magnetic refrigeration in low temperature range.

Keywords: rare-earth compound, magnetocaloric effect, metamagnetic transition

PACS: 71.20.Eh, 75.30Cr, 75.30.Sg **DOI:** 10.1088/1674-1056/25/12/127104

1. Introduction

The magnetic refrigeration based on magnetocaloric effect (MCE) is superior to the conventional gas compression-expansion refrigeration technique due to its higher energy transfer efficiency and environmental friendliness.[1–5] In recent years, the environmental degradation and the demand of new energy technique have aroused the passion of scientists to develop this advanced refrigeration technology and search for high-performance magnetocaloric materials, which exhibit large MCE, high refrigerant capacity (*RC*), and negligible hysteresis loss.[6–9]

In the past few decades, large MCEs have been reported in many materials with magnetic transition from ferromagnetic (FM) to paramagnetic (PM) states, in which a negative magnetic entropy change ΔS_M (conventional MCE) is obtained by applying a magnetic field. On the other hand, the antiferromagnetic (AFM) material exhibits positive magnetic entropy change ΔS_M (inverse MCE) with applying a magnetic field due to the disordering of AFM sublattices antiparallel to the magnetic field.[10,11] However, recently some AFM materials have also been found to exhibit large conventional MCEs, which are associated with the first-order field-induced metamagnetic transition from AFM to FM states.[12,13] Moreover, the AFM–FM metamagnetic transition shows perfect magnetic reversibility, so it is favorable for the practical application in magnetic refrigeration. These results hint us that large reversible MCE could be found not only in FM materials but also in AFM materials.

As one of the important rare-earth (R) based series, the ternary intermetallic RTX compounds (R = rare earth, T = transitional metal, X = p-block metal) have been investigated systematically in the past decades.[14–16] It is interesting to note that although the X atoms hardly contribute the magnetic moments, the crystallographic structure would vary with the change of X atoms, thus leading to the different magnetic and magnetocaloric properties of RTX compounds.[16] For example, the HoNiSi compound crystallizes in the orthorhombic TiNiSi-type structure and experiences an AFM–PM transition,[13] while the HoNiAl compound crystallizes in the hexagonal ZrNiAl-type structure and undergoes successive AFM–FM and FM–PM transitions.[17] Moreover, the HoNiIn compound also crystallizes into ZrNiAl-type structure as HoNiAl, but it shows successive spin-reorientation-like transition and FM–PM transition.[18] In order to further understand the effects of different p-block metals X on the magnetic and magnetocaloric properties in RTX compounds, in present work, we study the magnetic properties and MCE of HoNiGa compound in detail.

*Project supported by the National Natural Science Foundation of China (Grant Nos. 51671022 and 51427806), the Beijing Natural Science Foundation, China (Grant No. 2162022), and the Fundamental Research Funds for the Central Universities, China (Grant No. FRF-TP-15-002A3).

†Corresponding author. E-mail: zhanghu@ustb.edu.cn

© 2016 Chinese Physical Society and IOP Publishing Ltd

2. Experiment

The polycrystalline HoNiGa compound was prepared by arc-melting appropriate proportion of constituent components with the purity better than 99.9 wt%. The ingot was flipped over and melted several times to ensure homogeneity. The as-cast sample was wrapped in tantalum foil and annealed in a high-vacuum quartz tube at 1223 K for 3 weeks, and then quenched in ice water. The crystal structure was investigated by powder x-ray diffraction (XRD) at room temperature through using Cu Kα radiation, and the structure parameters were determined by Rietveld refinement[19] through using GSAS[20]/EXPGUI softwares.[21] The XRD investigation confirmed that HoNiGa compound crystallizes into a single phase with TiNiSi-type orthorhombic structure (space group *Pnma*). The lattice parameters obtained from Rietveld refinement as shown in Fig. 1 are $a = 6.8161(3)$ Å, $b = 4.2737(2)$ Å, and $c = 7.3242(3)$ Å, respectively, which are in good agreement with the data reported in previous literature.[22] The magnetic properties of the compound were measured by using a superconducting quantum interference device (model MPMS SQUID VSM) from Quantum Design, Inc.

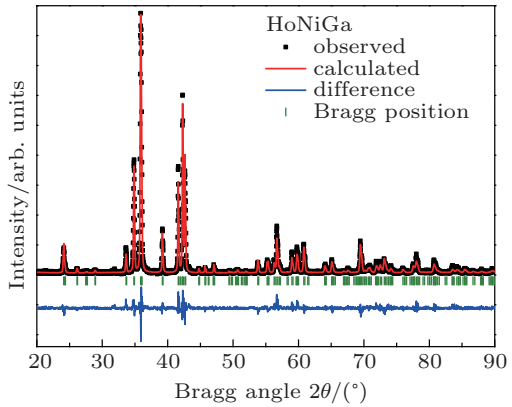


Fig. 1. (color online) Observed (dots) and calculated intensities (line drawn through the data points) of the fully refined x-ray diffraction pattern of HoNiGa compound at room temperature. The short vertical lines indicate the Bragg peak positions of the orthorhombic TiNiSi-type structure. The lower curve shows the difference between the observed and calculated intensities.

3. Results and discussion

The temperature (T) dependences of zero-field-cooling (ZFC) and field-cooling (FC) magnetization (M) for HoNiGa compound under a magnetic field of 0.01 T are shown in Fig. 2(a). It is found that the HoNiGa compound undergoes a magnetic transition from AFM to PM states around the Néel temperature $T_N = 10$ K with the increase of temperature. In addition, it is worth noting that neither thermal hysteresis nor discrepancy between ZFC and FC curves can be observed, indicating the perfect thermomagnetic reversibility of magnetic transition, which is beneficial to the practical application of magnetic refrigeration. The temperature dependence of the reciprocal of magnetic susceptibility (χ^{-1}) under 1 T is also displayed in Fig. 2(a), and the relation between χ^{-1} and temperature obeys the Curie–Weiss law in PM section. The paramagnetic Curie temperature (θ_p) and effective magnetic moment (μ_{eff}) of HoNiGa compound, determined by Curie–Weiss fit of χ^{-1}–T curve, are 13.3 K and 10.43 μ_B/Ho^{3+}, respectively. This calculated μ_{eff} value is close to the theoretical magnetic moment of holmium cation (Ho^{3+}: 10.60 μ_B), indicating that the magnetic moments of HoNiGa originate from Ho^{3+} while the Ni atoms hardly contribute the magnetic moments. This fact is consistent with many previous results about *RTX* compounds.[13,23,24] In addition, as is well known, the θ_p value represents the sum of all magnetic interactions in system, and usually an AFM material exhibits a negative θ_p value.[25] However, here the positive θ_p value indicates the presence of predominant FM interaction in HoNiGa compound under 1 T, so it suggests that the AFM ground state in HoNiGa is unstable and could be converted into an FM state by external magnetic field.

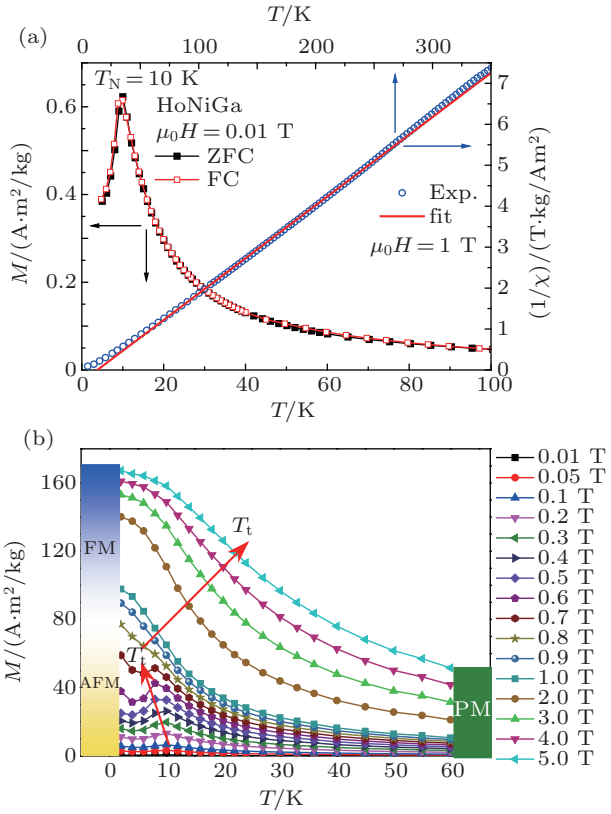


Fig. 2. (color online) (a) Temperature dependences of ZFC and FC magnetizations for HoNiGa under a magnetic field of 0.01 T and the inverse dc susceptibility (χ^{-1}) as a function of temperature fitted to Curie–Weiss law in a magnetic field of 1 T; (b) temperature dependences of magnetization for HoNiGa under various magnetic fields.

In order to further understand the effect of magnetic field on the phase transition, the temperature dependences of magnetization for HoNiGa compound under various applied fields are measured as shown in Fig. 2(b). The M–T curves at low magnetic fields each exhibit a typical λ-type peak around T_N, revealing that HoNiGa experiences an AFM–PM magnetic transition at low magnetic field. With the increase of magnetic field, the magnetization below T_N increases obviously,

indicating the occurrence of the field-induced metamagnetic transition from AFM to FM states. When the magnetic field is larger than 0.8 T, the HoNiGa compound shows a step-like behavior of M–T curve, corresponding to the typical characteristic of FM–PM magnetic transition.[26,27] Meanwhile, the magnetic transition becomes gentle with increasing magnetic field and the magnetization is still at high value in PM region under high magnetic fields. This fact implies the possible presence of field-induced short-range FM correlations in PM region.[17,25]

Figure 3(a) shows the magnetization isotherms of HoNiGa compound under applied fields up to 5 T in a temperature range of 2 K– 8 K. It is seen from the inset of Fig. 3(a) that the magnetization under low magnetic field increases with the increase of temperature, revealing the characteristic of AFM ground state. With the increase of magnetic field, a sharp jump of magnetization occurs when the field reaches a critical value (e.g., 0.5 T at 2 K), which leads to a crossover of magnetization isotherms. Then, the magnetization decreases gradually with increasing temperature, corresponding to the characteristic of FM state. This result confirms that the AFM ground state in HoNiGa exhibits a weak stability and can be converted into FM state by applying an external field, which is consistent with the discussion of positive θ_p value. In addition, the saturation magnetic moment (μ_S), obtained by extrapolating the M–$1/\mu_0 H$ curve to $1/\mu_0 H \to 0$ through using M–$\mu_0 H$ curve at 2 K, is 9.56 μ_B/Ho^{3+}, which is close to the theoretically calculated gJ value of 10.00 μ_B/Ho^{3+}. This large μ_S value is attributed to the field-induced metamagnetic transition from AFM to FM states. On the other hand, it is seen from Fig. 3(b) that the magnetization changes remarkably around $T_N = 10$ K. Therefore, the high μ_S of field-induced FM phase and the large change of magnetization around the transition temperature imply the possibility of high MCE in HoNiGa compound.[1,24] In addition, the magnetization isotherms at temperatures higher than T_N (up to 33 K) still show distinct curvatures as shown in Fig. 3(b), further confirming the presence of short-range FM correlations in PM region. As is well known, the magnetic hystereses in the magnetizing and demagnetizing processes will reduce the effective refrigerant capacity (RC) of magnetic material.[28] Here, the M–$\mu_0 H$ curves are measured in the field increasing and decreasing modes, and no magnetic hysteresis is observed. This perfect reversibility of magnetic transition is desirable for practical applications in magnetic refrigeration.

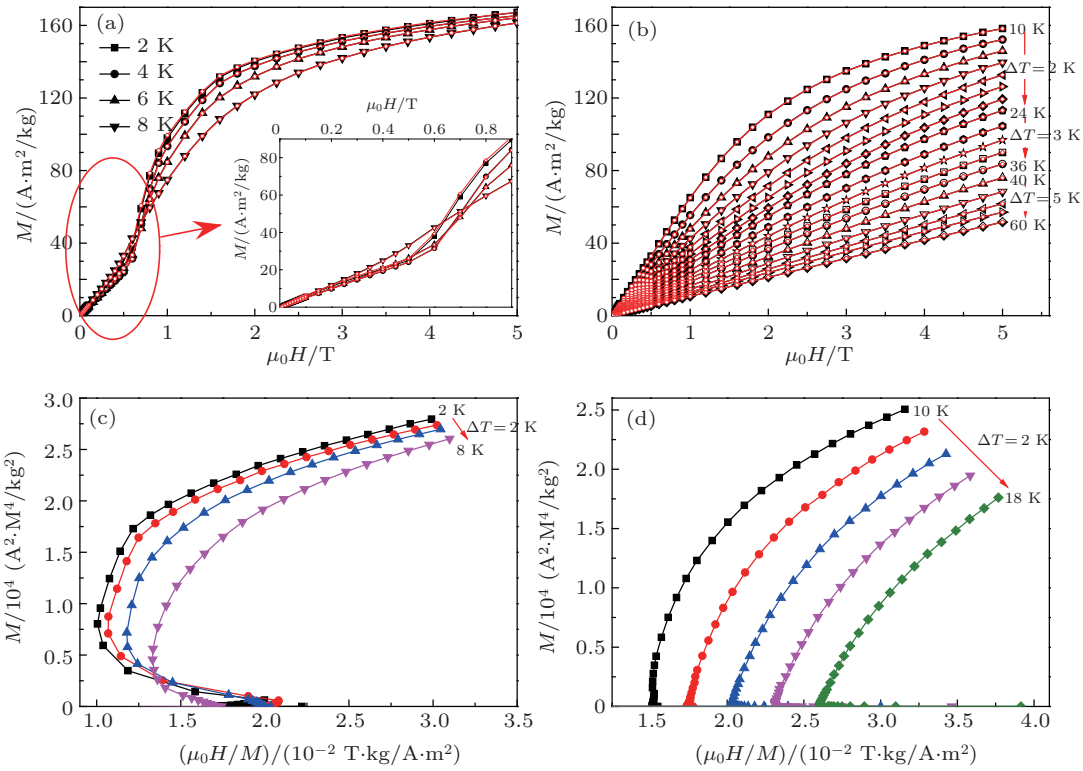


Fig. 3. (color online) Magnetization isotherms of HoNiGa compound in the temperature regions of (a) 2 K–8 K and (b) 10 K–60 K, respectively. The inset of Fig. 3(a) shows the magnetization isotherms under relatively low magnetic fields. The Arrott plots of HoNiGa compound are in the temperature regions of (c) 2 K–8 K and (d) 10 K–18 K, respectively.

The Arrott plots are derived from the M–$\mu_0 H$ curves and are presented in Figs. 3(c) and 3(d). According to Banerjee criterion, a magnetic transition is expected to be of first-order when the Arrott plot exhibits negative slope or inflection point; otherwise it is considered as second-order when the slope of Arrott plot is positive.[29] It is seen that the Arrott plots below T_N show obvious negative slopes, confirming that the field-induced AFM–FM metamagnetic transition is of first-order. On the other hand, the positive slope of Arrott plot above T_N proves the characteristic of a second-order magnetic transition

from PM state to FM state.

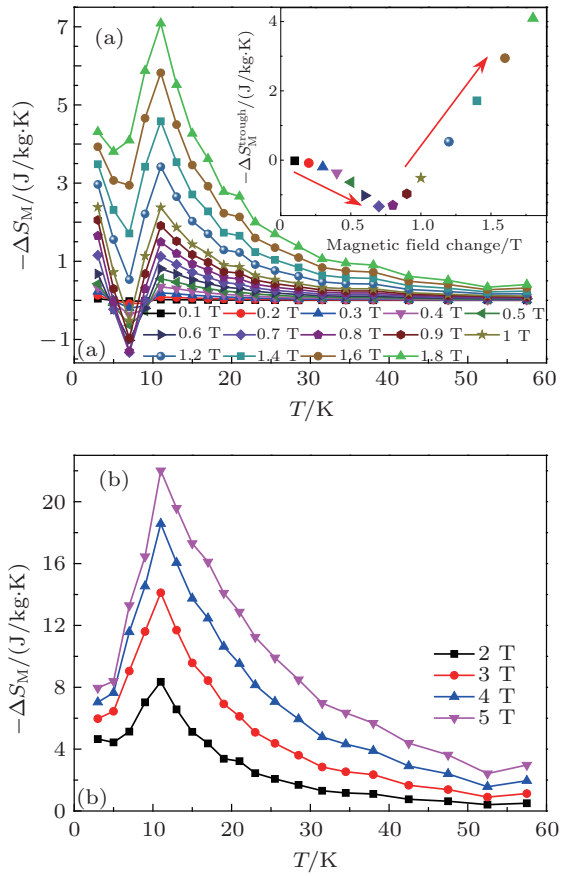


Fig. 4. (color online) (a) Temperature dependences of magnetic entropy change $-\Delta S_M$ for HoNiGa compound under different magnetic field changes from 0.1 T to 1.8 T. The inset shows the $-\Delta S_M$ through value below T_N as a function of magnetic field change. (b) Temperature dependences of magnetic entropy change $-\Delta S_M$ for HoNiGa compound under different magnetic field changes increasing from 2 T to 5 T.

The ΔS_M values for different magnetic field changes are calculated from magnetization isotherms by using Maxwell relation:

$$\Delta S_M(T,H) = \mu_0 \int_0^H (\partial M/\partial T)_H \mathrm{d}H, \tag{1}$$

and the obtained results are plotted in Fig. 4. It is found from Fig. 4(a) that small negative $-\Delta S_M$ values (inverse MCE) can be observed below T_N for relatively low magnetic field change, which is due to the presence of AFM state at low temperatures. The inset of Fig. 4(a) shows the $-\Delta S_M$ trough value below T_N as a function of magnetic field change. It is clearly seen that at first the $-\Delta S_M$ trough value decreases with the increase of magnetic field and reaches a minimum value of -1.33 J/kg for a field change of 0.7 T, which is due to the more disordered AFM magnetic sublattices antiparallel to the applied magnetic field. Then, the negative $-\Delta S_M$ value starts to increase when the $\Delta\mu_0 H > 0.7$ T, and it gradually changes to positive value. Such a sign change of $-\Delta S_M$ value is due to the field-induced metamagnetic transition from AFM to FM states.[30]

With the further increase of magnetic field, a large positive $-\Delta S_M$ peak (normal MCE) of -22.0 J/kg K can be found around the transition temperature for a field change of 5 T (Fig. 4(b)). This giant MCE is related to the high saturation magnetic moment of field-induced FM phase and the rapid change of magnetization around the transition temperature.[24] Meanwhile, it is interesting to note that the $-\Delta S_M$ peak broadens asymmetrically towards higher temperatures with increasing field, which is likely to be related to the presence of field-induced FM correlation in PM region.[31] As another important parameter to quantify the heat transferred from hot to cold sinks during an ideal refrigeration cycle, the *RC* value is estimated from the following formula:

$$RC = \int_{T_1}^{T_2} |\Delta S_M| \mathrm{d}T, \tag{2}$$

where T_1 and T_2 are the temperatures corresponding to both sides of the half maximum $-\Delta S_M$ peak. The *RC* reaches a value as high as 279 J/kg for a magnetic field change of 5 T. For comparison, Table 1 summarizes the MCEs of HoNiGa and some other magnetocaloric materials with similar magnetic transition temperatures. It can be seen that the $-\Delta S_M$ and *RC* values of HoNiGa are comparable to or even larger than those of some other magnetic refrigerant materials in the same temperature range.

Table 1. Magnetocaloric properties of HoNiGa and some other magnetocaloric materials with similar transition temperatures.

Materials	T_C/T_N/K	$-\Delta S_{Mmax}$/(J/kg·K)		*RC*/(J/kg) (5 T)	Refs.
		2 T	5 T		
TbCuSi	11	2.7	10.0	246	[32]
$Eu_8Ga_{16}Ge_{30}$	13	4.5	–	400	[33]
$Dy_{0.9}Tm_{0.1}Ni_2B_2C$	9.2	4.05	14.7	220[a]	[34]
$ErNi_5$	9	–	15.0	232[a]	[35]
ErNiIn	9	10.1	15.1	229	[18]
$DyNi_2B_2C$	10.5	4.4	17.6	186[a]	[36]
HoCoAl	10	12.5	21.5	437[a]	[37]
HoCuAl	11.2	17.5	30.6	486	[38]
DyCuSi	10	10.5	24.0	381	[39]
HoNiGa	10	8.4	22.0	279	This work

[a]The *RC* values are estimated from the temperature dependence of ΔS_M in the literature.

According to the mean-field approximation, despite the diversities in the shape of $-\Delta S_{\rm M}$–T curve for different materials, the field dependences of $-\Delta S_{\rm M}$ for all the materials with second-order magnetic transition can be expressed as

$$|\Delta S_{\rm M}^{\rm pk}| \propto H^n, \tag{3}$$

where the local exponent n is 2/3 at the transition temperature.[40] Therefore, it is considered to be an effective method to investigate the nature of magnetic transition. The $\mu_0 H^{2/3}$ dependence of $|\Delta S_{\rm M}^{\rm pk}|$ value and the linear fitting are plotted in Fig. 5. It is clearly seen that the $\mu_0 H^{2/3}$ dependence of $|\Delta S_{\rm M}^{\rm pk}|$ well follows the linear fitting with a fit index of 0.9934. The slight deviation of $|\Delta S_{\rm M}^{\rm pk}|$ at 1 T might be related to the presence of a small number of AFM components under relatively low magnetic field.[41] This result indicates that the field dependence of $\Delta S_{\rm M}$ for HoNiGa can be expressed well by the mean-field approximation, thus further proving that the HoNiGa undergoes a second-order FM–PM magnetic transition under high magnetic field.

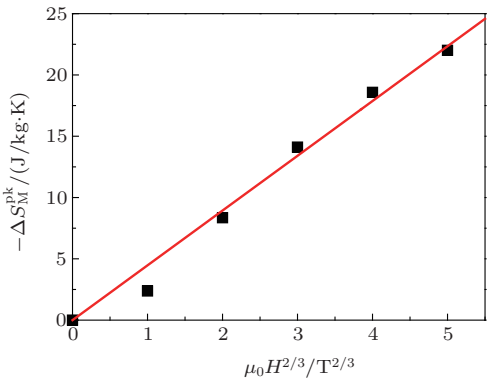


Fig. 5. (color online) The $|\Delta S_{\rm M}^{\rm pk}|$ value as a function of $\mu_0 H^{2/3}$ and the linear fitting to it.

4. Conclusions

In summary, the HoNiGa compound undergoes an AFM–PM magnetic transition under low magnetic field in the vicinity of $T_{\rm N} = 10$ K. However, the AFM ground state can be converted into FM state due to its weak stability, and thus the HoNiGa undergoes a second-order FM–PM magnetic transition under high magnetic field. Moreover, perfect thermal and magnetic reversibility are observed in HoNiGa, and it is desirable for the practical applications in magnetic refrigeration. The field-induced FM phase exhibits a high saturation magnetic moment and a large change of magnetization around the transition temperature, thus leading to a large MCE. Besides, the field dependence of $|\Delta S_{\rm M}^{\rm pk}|$ for HoNiGa can be expressed well by mean-field approximation, and thus it confirms the nature of second-order FM–PM magnetic transition under high magnetic field. Consequently, the large MCE without thermal and magnetic hysteresis makes HoNiGa compound a promising candidate for magnetic refrigeration materials in low temperature range.

References

[1] Tishin A M and Spichkin Y I 2003 *The Magnetocaloric Effect and its Application* (IOP Publishing)
[2] Shen B G, Hu F X, Dong Q Y and Sun J R 2013 *Chin. Phys. B* **22** 017502
[3] Yue M, Zhang H G, Liu D M and Zhang J X 2015 *Chin. Phys. B* **24** 017505
[4] Tegus O, Bao L H and Song L 2013 *Chin. Phys. B* **22** 037506
[5] Wang D H, Han Z D, Xuan H C, Ma S C, Chen S Y, Zhang C L and Du Y W 2013 *Chin. Phys. B* **22** 077506
[6] Franco V, Blázquez J S, Ingale B and Conde A 2012 *Ann. Rev. Mater. Res.* **42** 305
[7] Liu J 2014 *Chin. Phys. B* **23** 047503
[8] Li L W 2016 *Chin. Phys. B* **25** 037502
[9] Zhang D K, Zhao J L, Zhang H G and Yue M 2014 *Acta Phys. Sin.* **63** 197501 (in Chinese)
[10] Samanta T, Das I and Banerjee S 2007 *Appl. Phys. Lett.* **91** 152506
[11] Zuo W L, Hu F X, Sun J R and Shen B G 2015 *Chin. Phys. B* **24** 097104
[12] Chen J, Shen B G, Dong Q Y, Hu F X and Sun J R 2010 *Appl. Phys. Lett.* **96** 152501
[13] Zhang H, Wu Y Y, Long Y, Wang H S, Zhong K X, Hu F X, Sun J R and Shen B G 2014 *J. Appl. Phys.* **116** 213902
[14] Jang D, Gruner T, Steppke A, Mitsumoto K, Geibel C and Brando M 2015 *Nat. Commun.* **6** 8680
[15] Gupta S and Suresh K G 2015 *J. Alloys Compd.* **618** 562
[16] Zhang H and Shen B G 2015 *Chin. Phys. B* **24** 127504
[17] Singh N K, Suresh K G, Nirmala R, Nigam A K and Malik S K 2007 *J. Appl. Phys.* **101** 093904
[18] Zhang H, Xu Z Y, Zheng X Q, Shen J, Hu F X, Sun J R and Shen B G 2011 *J. Appl. Phys.* **109** 123926
[19] Rietveld H M 1967 *Acta Crystallogra* **22** 151
[20] Larson A C and Von Dreele R B 1994 *Document LAUR* 86
[21] Toby B H 2001 *J. Appl. Crystallogr.* **34** 210
[22] Dwight A E 1967 in *Proc. 6th Rare Earth Resaerch Conf.*, Oak Ridge Laboratories, Tennessee, p. 156
[23] Semitelou I and Kotsanidis P 1991 *J. Magn. Magn. Mater.* **102** 67
[24] Zhang H, Shen B G, Xu Z Y, Shen J, Hu F X, Sun J R and Long Y 2013 *Appl. Phys. Lett.* **102** 092401
[25] Mallik R, Sampathkumaran E V and Paulose P L 1998 *Solid State Commun.* **106** 169
[26] Ahn K, Pecharsky A O, Gschneidner K A Jr and Pecharsky V K 2005 *J. Appl. Phys.* **97** 063901
[27] Shen J, Zhang H and Wu J F 2011 *Chin. Phys. B* **20** 027501
[28] Provenzano V, Shapiro A J and Shull R D 2004 *Nature* **429** 853
[29] Banerjee B K 1964 *Phys. Lett.* **12** 16
[30] Gschneidner K A Jr, Pecharsky V K and Tsokol A O 2005 *Rep. Prog. Phys.* **68** 1479
[31] Arora P, Chattopadhyay M K, Sharath Chandra L S, Sharma V K and Roy S B 2011 *J. Phys.: Condens. Matter* **23** 056002
[32] Chen J 2010 "Magnetic properties and magnetocaloric effects in Ni2In-type RCuSi and CrB-type *R*Ga compounds", Ph. D. Thesis (Graduate University of Chinese Academy of Sciences) (in Chinese)
[33] Chaturvedi A, Stefanoski S, Phan M H, Nolas G S and Srikanth H 2011 *Appl. Phys. Lett.* **99** 162513
[34] Li L W and Nishimura K 2009 *Appl. Phys. Lett.* **95** 132505
[35] Von Ranke P J, Mota M A, Grangeia D F, Carvalho A M G, Gandra F C G, Coelho A A, Caldas A, de Oliveira N A and Gama S 2004 *Phys. Rev. B* **70** 134428
[36] Li L W, Nishimura K, Kadonaga M, Qian Z and Huo D 2011 *J. Appl. Phys.* **110** 043912
[37] Zhang X X, Wang W F and Wen G H 2001 *J. Phys.: Condens. Matter* **13** L747
[38] Wang L C, Dong Q Y, Mo Z J, Xu Z Y, Hu F X, Sun J R and Shen B G 2013 *J. Appl. Phys.* **114** 163915
[39] Chen J, Shen B G, Dong Q Y and Sun J R 2010 *Solid State Commun.* **150** 1429
[40] Oesterreicher H and Parker F T 1984 *J. Appl. Phys.* **55** 4334
[41] Yang L H, Zhang H, Hu F X, Sun J R, Pan L Q and Shen B G 2014 *J. Alloys Compd.* **596** 58